Reconstructing oxygen deficiency in the glacial Gulf of Alaska: Combining biomarkers and trace metals as paleo-redox proxies

Article *in* Chemical Geology · September 2020

DOI: 10.1016/j.chemgeo.2020.119864

12 authors, including:

Mark Zindorf
Institut Français de Recherche pour l'Exploitation de la Mer
7 PUBLICATIONS **0** CITATIONS
SEE PROFILE

Michelle Penkrot
University of Florida
8 PUBLICATIONS **6** CITATIONS
SEE PROFILE

Helen M. Talbot
Newcastle University
157 PUBLICATIONS **3,094** CITATIONS
SEE PROFILE

Maureen H. Walczak
Oregon State University
54 PUBLICATIONS **429** CITATIONS
SEE PROFILE

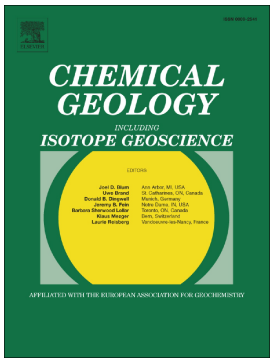

Reconstructing oxygen deficiency in the glacial Gulf of Alaska: Combining biomarkers and trace metals as paleo-redox proxies

Mark Zindorf, Darci Rush, John Jaeger, Alan Mix, Michelle L. Penkrot, Bernhard Schnetger, Frances R. Sidgwick, Helen M. Talbot, Cees van der Land, Thomas Wagner, Maureen Walczak, Christian März

PII: S0009-2541(20)30403-4

DOI: https://doi.org/10.1016/j.chemgeo.2020.119864

Reference: CHEMGE 119864

To appear in: *Chemical Geology*

Received date: 8 March 2020

Revised date: 27 August 2020

Accepted date: 1 September 2020

Please cite this article as: M. Zindorf, D. Rush, J. Jaeger, et al., Reconstructing oxygen deficiency in the glacial Gulf of Alaska: Combining biomarkers and trace metals as paleo-redox proxies, *Chemical Geology* (2020), https://doi.org/10.1016/j.chemgeo.2020.119864

Reconstructing oxygen deficiency in the glacial Gulf of Alaska: Combining biomarkers and trace metals as paleo-redox proxies

Mark Zindorf[1]*, Darci Rush[2], John Jaeger[3], Alan Mix[4], Michelle L. Penkrot[3], Bernhard Schnetger[5], Frances R. Sidgwick[6], Helen M. Talbot[7], Cees van der Land[1], Thomas Wagner[8], Maureen Walczak[4], Christian März[9]

[1] School of Natural and Environmental Sciences, Newcastle University, Newcastle upon Tyne, NE1 7RU, United Kingdom

* Current address/address of communication: Ifremer - Centre de Brest, Laboratoire Environnement Profond, 13 Technopôle Brest-Iroise BP 70, 29280 Plouzané, France

[2] Department of Marine Microbiology and Biogeochemistry, NIOZ Royal Netherlands Institute for Sea Research, and Utrecht University, Den Burg, P.O. Box 59 1790 AB, The Netherlands

[3] Department of Geological Sciences, University of Florida, Gainesville, FL 32611-2120, USA

[4] College of Earth, Ocean, and Atmospheric Sciences, Oregon State University, Corvallis, OR 97331-5503, USA

[5] Institut für Chemie und Biologie des Meeres (ICBM), Universität Oldenburg, D-26129 Oldenburg, Germany

[6] Medical School, Newcastle University, Newcastle upon Tyne, NE1 7RU, United Kingdom

[7] Department of Archaeology, University of York, YO10 5NG, York, United Kingdom

[8] The Lyell Centre, School of Energy Geoscience Infrastructure and Society, Heriot-Watt University, EH14 4HS Edinburgh, United Kingdom

[9] School of Earth and Environment, University of Leeds, LS2 9JT Leeds, United Kingdom

Keywords

Oxygen Deficient Zone; Anammox; BHT-*x* biomarker; Trace element redox proxies; Gulf of Alaska; IODP

Abstract

Marine anaerobic oxidation of ammonium (anammox) plays a central role in the nitrogen cycle of modern Oxygen Deficient Zones (ODZs). The newly developed bacteriohopanetetrol stereoisomer (BHT-*x*) biomarker for anammox, which is largely unaffected by early diagenesis, allows for the reconstruction of the presence and dynamics of past ODZs from the sedimentary record of continental margins. In this study, we investigate the development and dynamics of the ODZ in the Gulf of Alaska (GOA) between 60 and 15 cal ka BP using records of redox sensitive trace metals (TM) and the BHT-*x* anammox biomarker from IODP Site U1419 (~700 m water depth). The biomarker record indicates that the ODZ in the GOA was in concert with global climate fluctuations in the late Pleistocene. Anammox was more pronounced during warmer periods and diminished during cooler periods, as indicated by correlation with the $\delta^{18}O$ signal obtained by the North Greenland Ice core Project (NGRIP). Trace metal enrichments, however, do not match the trend in BHT-*x*. Systematic metal enrichments in intervals where biomarkers point to more intense water column deoxygenation are not observed. We suggest that this proxy discrepancy was caused by environmental factors, other than water column redox conditions, with opposing effects on the TM and biomarker records. Two of the most widely used redox indicators, Mo and U, are not significantly enriched throughout the sediment record at Site U1419. Site U1419 experienced some of the highest sedimentation rates (100 – 1000 cm ka^{-1}) ever reported for late Pleistocene continental margin sediments, leading to a continuous and rapid upward

migration of the sediment-water interface. We suggest that despite water column and seafloor oxygen depletion, significant sedimentary enrichments of these redox sensitive trace metals were prevented by a limited time for their diffusion across the sediment-water interface and subsequent enrichment as authigenic phases. Thus, depositional conditions were ideal for biomarker preservation but prevented significant authigenic trace metal accumulations. Similar discrepancies between organic and inorganic redox proxies could exist in other high sedimentation rate environments, potentially putting constraints on paleo-redox interpretations in such settings if they are based on trace metal enrichments alone.

1. Introduction

Along continental margins, oxygen deficient zones (ODZs) are established in a water mass when oxygen demand by organic matter re-mineralization exceeds oxygen re-supply by ventilation or mixing. At present, these conditions are common in restricted/stratified basins or estuaries, but also in western boundary current upwelling areas (e.g., off the western coasts of Africa, India, and the Americas; Paulmier and Ruiz-Pino, 2009).

Oxygen limitation can lead to reduced organic matter remineralization in the water column followed by the enhanced preservation and burial of organic matter in sediments underlying an ODZ (Hedges and Keil, 1995; Hartnet et al., 1998). As such, ODZs can play a key role in the global carbon cycle through the long-term burial of carbon from the ocean-atmosphere system in sediments (Devol and Hartnett, 2001) and dark carbon fixation (Lengger et al., 2019).

The increase in sea surface temperature predicted with global climate change will reduce oceanic oxygen uptake (e.g., Shaffer et al., 2009; Breitburg et al., 2018). Existing ODZs are also projected to intensify in the future (Oschlies et al., 2008; Pachauri et al., 2014). These changes are expected to have severe impacts on both humans (e.g., decreased fish stock;

Gilly et al., 2013) and global biogeochemical cycles (e.g., by increasing organic carbon burial; Devol and Hartnett, 2001). To assess how ODZs might behave under future climatic conditions, it is essential to understand their response to past climate change.

In addition to their importance in the global carbon cycle, ODZs play an important role in the global nitrogen (N) cycle. The removal of bioavailable N species has been shown to be significantly enhanced under low O_2 conditions (Codispoti et al., 2001; Lam and Kuypers, 2011). Anaerobic ammonium oxidation (anammox) is a process by which specific bacteria (i.e. anammox bacteria) use nitrite (NO_2^-) to oxidize ammonium (NH_4^+) to dinitrogen gas (N_2), which is subsequently lost from the ocean to the atmosphere (Van de Graaf et al., 1995; Mulder et al., 1995). The anammox process occurs in anoxic marine sediments and ODZs (Kuypers et al., 2003; Hamersley et al., 2007; Lam and Kuypers, 2011; Pitcher et al., 2011), and it has been proposed to account for 29 % of total oceanic N loss (Ward, 2013). Anammox bacteria are inhibited by the presence of oxygen. Dalsgaard et al. (2014) report 50% inhibition at ~900 nM O_2, Kalvelage et al. (2012) and Bristow et al. (2016) report the O_2 limit for anammox at 10-20 µM. Thus, molecular evidence of anammox recorded in marine sediment cores can be used as a proxy for oxygen depletion to reconstruct past ODZ dynamics.

The modern Gulf of Alaska (GOA) exhibits a seasonal ODZ between 670 and 1060 m water depth where annually averaged O_2 concentrations fall below 0.5 ml O_2 L^{-1} (Figure 1) (Moffitt et al., 2015). Under current climatic conditions, this ODZ is most pronounced during spring and autumn, decreases in intensity in winter, and disappears during summer (Paulmier and Ruiz-Pino, 2009). While the present behavior of the ODZ in the GOA is well-constrained, its intensity during the last glacial cycle is not fully constrained. For the wider Northeastern Pacific area, ODZ paleo-records exist back to ~70 ka (e.g. offshore California; Cannariato and Kennett, 1999; Zheng et al., 2000; Cartapanis et al., 2011). However, north of Vancouver

Island, where the GOA is situated, the oxygen deficiency record is only resolved for the last 17 ka (McKay et al., 2005; Barron et al., 2009; Davies et al., 2011; Addison et al., 2012). Thus, no data exist for the Last Glacial Maximum (LGM, 33 - 26.5 ka BP, Clark et al., 2009) nor the preceding interglacial period (Marine Isotope Stage 3, 57-29 ka BP, Lisiecki and Raymo, 2005).

Earlier studies (Cannariato and Kennett, 1999; Cartapanis et al., 2011) suggest that the North Pacific ODZ expanded during warmer periods (e.g. Bølling-Al'erød (B/A; 13.7 - 12.7 ka BP), early Holocene (<11.7 ka BP)), and was less intense, less extensive, or not present during cooler periods (e.g. LGM, Younger Dryas (YD; 12.7 - 11.7 ka BP)). It is not yet fully understood what caused these temporal ODZ fluctuations. Favored mechanisms include increased upwelling along the California margin that fueled primary productivity and thus oxygen consumption, and/or increased water column stratification caused by changing ocean circulation in the northern North Pacific (McKay et al., 2005).

Reconstructions of the North Pacific and GOA ODZ intensities have been based on the accumulation of redox sensitive trace metals (TM) (Zheng et al., 2000; Cartapanis et al., 2014), the abundances of benthic foraminifera (Bernhard and Reimers, 1991; Cannariato and Kennett, 1999; Ohkushi et al., 2013), and the occurrence of laminated sediments (Emery and Hülsermann, 1961; Ortiz et al., 2004; Davies et al., 2011). TM can either precipitate as sulfides (or co-precipitate with pyrite) in the presence of H_2S in sulfidic waters (i.e. Cu, Mo, Ni), or form less soluble species in sub- or anoxic waters (i.e. Cr, V and U; review by Calvert and Pedersen, 2007). However, only one study in the North Pacific ODZ uses biomarker lipids (stanol to sterol ratios) as redox proxies (Nakakuni et al., 2017).

Ladderane lipids have been identified as diagnostic biomarker lipids for anammox (e.g., Sinninghe Damsté et al., 2002; Kuypers et al., 2003; Jaeschke et al., 2009a; Jaeschke et al.,

2009b). However, ladderanes are relatively labile and rarely preserve over long timescales in the sedimentary record (Rush et al., 2012). Bacteriohopanepolyols (BHP), pentacyclic triterpenoids that are synthesized by bacteria, have been used as biomarkers (Rohmer et al., 1984) for specific processes and environmental conditions (e.g., cyanobacterial oxygenic photosynthesis, Summons et al., 1999; general methanotrophy, Talbot et al., 2001; methanotrophy in peat moss, van Winden et al., 2012 and aerobic water column methanotrophy, Berndmeyer et al., 2013). Recently, anammox bacteria were found to synthesize bacteriohopanetetrol (BHT-34*S*) and its stereoisomer BHT-*x* (Rush et al., 2014). BHT-34*S* is ubiquitous in marine sediments and is produced by a diverse range of bacterial genera (Rohmer et al., 1984; Talbot et al., 2007a; Talbot and Farrimond, 2007). However, the marine anammox genus '*Candidatus Scalindua*' is the only known source of BHT-*x* (Schwarz-Narbonne et al., 2020). BHT-*x* has already been used as a biomarker for anammox in ODZ settings (i.e., Chilean Margin, Mayr et al., 2017; Arabian Sea ODZ, Lengger et al., 2019; Mediterranean sapropels, Rush et al., 2019). The ratio between BHT-*x* and total BHT can be used to determine the contribution of anammox bacteria relative to all BHT-producing bacteria in marine environments (Sáenz et al., 2011). The generally good preservation of BHPs (Talbot et al., 2016; van Dongen et al., 2006) favors the use of BHT-*x* in deeper/older sediments, and BHT-*x* biomarker can be used as an alternative biomarker to ladderanes to infer the presence of ODZs in the geological past.

This study is the first to combine BHT-*x* biomarker data with inorganic TM redox and bioproductivity proxies to establish a record of past ODZ dynamics in the GOA, back to ~60 ka BP. We directly compare different organic and inorganic redox proxies and present a new BHT-*x* record to demonstrate the potential of the new biomarker proxy, provide a note of caution against the uncritical use of certain TM records in very high sedimentation rate settings, and discuss how oxygen depletion in the GOA was linked to late Pleistocene climate

cycles.

2. Methods

For this study, sediment samples from IODP Expedition 341, Site U1419 in the Gulf of Alaska (Figure 1) have been used. Site U1419 is located in 721 m water depth on the continental slope above the Khitrov basin (See Figure 1). Five holes (A-E) were drilled (average recovery 82 %) yielding a composite core length of 177 m (Jaeger et al., 2014). All depth information in this paper will be given in mbsf (meters below sea floor) on the CCSF-B depth scale (Composite Coring depth below Sea Floor), a composite depth scale combining all drilled holes at the same site and corrected for sediment expansion (Jaeger et al., 2014).

2.1 Age determination

The age model for U1419 between the present and ~54.0 cal ka BP is from Walczak et al. (in press) and is based on 250 ^{14}C dates on both benthic and planktic foraminifera; beyond ~54.0 cal ka BP, sedimentation rates are constrained by two tie points derived from δ^{18}O correlation to Hulu Dongge at ~59.3 and 61.5 cal ka BP. Radiocarbon dates were calibrated with the IntCal13 curve (Reimer et al., 2013). A variable planktonic reservoir correction (R) (average 370 a +/- 350 a) was used, based on a simple one-dimensional vertical circulation box model and the measured benthic - planktonic (B-P) differences in the core. Benthic foraminifera ages were calibrated using a constant benthic ΔR of 1200 +/- 600 a reflecting the root mean square error of the propagated combination of planktic and B-P errors. All constraints were evaluated using the Bayesian age model program BChron (Haslett and Parnell, 2008); the resulting age model has an average 1-σ uncertainty of 210 cal a with maximum uncertainty of ~700 cal a between 55.0 - 60.0 cal ka BP. Further details of the age model are available in Walczak et al. (in press).

2.2 Sampling strategy

A total of 114 sediment samples were taken (on board and during the post-cruise sampling party) at an average depth resolution of ~1.3 m. The investigated sediment record spans the time period between 15 and 60 cal ka BP (6 – 100 m CCSF-B) because the age model for this segment has been constrained and a continuous sample coverage exists. All samples were freeze-dried and homogenized using an agate mortar and pestle or an agate ball mill.

All 114 samples were analyzed for Al and trace metals (Cr, Cu, Ni and V), 91 samples were analyzed for U. A subset of 55 samples was analyzed for BHDs, total organic carbon (TOC) and 23 out of these 55 samples were analyzed for K, Mg, Mo and Si.

2.3 Anammox biomarker

2.3.1 Lipid Extraction

Lipids were extracted using a modified Bligh and Dyer extraction (Bligh and Dyer, 1959; Cooke et al., 2009). Briefly, ~3 g of freeze-dried sediment was extracted using 19 ml of a H_2O/MeOH/chloroform solution (4:10:5, v:v:v). This mixture was sonicated for 15 min at 40˚C and centrifuged at 12,000 rpm for 15 min. The supernatant was collected and the extraction procedure was repeated twice. Then, the chloroform and the aqueous phase in the supernatant were separated by adding water until a H_2O:MeOH ratio of 1:1 (v:v) was reached. The chloroform phase containing the total lipid extract was removed and this step was repeated twice. The Bligh-Dyer extract was subsequently dried by rotary evaporation.

A known amount of 5α-pregnane-3ß,20ß-diol internal standard was added to the extracts. They were then acetylated in 0.5 ml of 1:1 (v:v) acetic anhydride and pyridine mixture for 1h at 50˚C, then overnight at room temperature. For liquid chromatography analysis, the lipid extracts were dissolved in 1ml MeOH/propan-2-ol (60:40 v:v).

2.3.2 Lipid analyses

BHPs were analyzed by high performance liquid chromatography coupled to positive ion atmospheric pressure chemical ionization mass spectrometry HPLC/APCI-MS^n (Talbot et al., 2007). The coefficient of variation of this method was 20% checked on triplicate analyses of every 10^{th} sample. However, one triplicate analysis with very low BHT content caused a coefficient of variation of 42%. A triplicate extraction of one sample yielded a coefficient of variation of 7%.

To address the possibility of a terrestrial source of organic matter, lipid extracts were screened for soil marker BHPs (Zhu et al., 2011). These compounds were only found in low abundance below quantification limit in 4 samples, indicating the majority of BHPs in these samples derived from a marine source. It should be noted that the HPLC method used in this study does not separate BHT-*x* from another stereoisomer of BHT, BHT-34*R* (Kusch et al. 2018; Schwartz-Narbonne et al., 2020). However, there are no known marine bacterial sources of BHT-34*R* (see Rush et al. 2014) and to the best of our knowledge BHT-34*R* has not been detected in a marine setting. As this Gulf of Alaska record does not appear to be influenced by the input of terrestrial BHPs, we expect the peak of BHT isomer in these samples to be BHT-*x*. Nevertheless, we cannot discount that it might include BHT-34*R*. Here we discuss the abundances of BHT-34*S* and BHT-*x* as a proxy for anammox and the absence of oxygen in the GOA ODZ from 60 to 15 ka.

Oxygen deficient conditions generally lead to better preservation of OM (Burdige, 2007). Thus, caution should be taken when applying biomarkers in sediments underlying ODZs (Jaeschke et al 2009b). To avoid this potential preservation bias, BHT-*x* and BHT-34*S* abundances were normalized to TOC and reported as a ratio of BHT-*x* to total BHT (BHT-*x*/BHTtot). We assume that BHT-34*S* and BHT-*x* are affected in the same way by degradation processes. The ratio between BHT-*x* and total BHT therefore is a robust proxy for marine anammox.

2.4 Inorganic geochemistry

Two independent methods for bulk element geochemistry analyses (i.e. wavelength-dispersive X-ray fluorescence (XRF) and inductively coupled plasma mass spectrometry (ICP-MS)) were applied to our samples. We combined results from both to have a robust dataset with increased sample resolution. Comparability of the data was established by co-plotting and comparison of average data.

For 23 samples, wavelength-dispersive XRF (Panalytical Axios max, 3 kW) was used to analyze the contents of Al, Ca, Cr, Cu, K, Mg, Mo, Ni, Si and V. 700 mg of sample were mixed with 4200 mg di-lithiumtetraborate, pre-oxidized with 1 g ammonium nitrate at 500 °C, and fused at 1400 °C to homogenous glass beads. Root mean squared error of this method was <1 % for all major elements and <10 ppm for all minor elements except Ni (13 ppm). Precision for the inhouse standard was <0.5 rel% for all major and <10 rel% for all minor elements.

For 91 samples, Al and minor elements (Cr, Cu, Ni, U and V) were measured via an Element 2 ICP-MS (Kamenov et al., 2009; Penkrot et al., 2018a). Analytical uncertainty is better than ±5 % for all elements.

Where one element was analyzed by both XRF and ICP-MS (Al, Cr, Cu, Ni and V), the results are combined into one dataset. Comparability of the analysis has been established by comparing averages and co-plotting results of individual elements.

TOC was analyzed using a Leco combustion analyzer. Reproducibility was better than 5 % as checked on duplicates of every 10^{th} sample.

XRF, ICP-MS and Leco data are presented as weight percent or weight parts per million of dry sediment (wt% or ppm) or element/Al ratios (wt%/wt% or ppm/wt%). Also mass accumulation rates have been calculated for individual trace elements based on the formula:

AR_{TM} (mg cm^{-2} ka^{-1}) = (TM (wt%)/100)*(sedimentation rate*dry bulk density). The dry bulk density for each sample was taken from a linear regression through shipboard dry bulk density data from Jaeger et al. (2014).

3. Results

3.1 Age model

The core has an age of ~59 cal ka BP at 100 mbsf (Walczak et al., in press). The age model has been used to calculate sedimentation rates for the investigated interval. Sedimentation rates are around 50 cm ka^{-1} in the top 6 m of the core, representing the last ~17 ka (Figure 2). The deglacial section exhibits highest sedimentation rates exceeding 2500 cm ka^{-1}. In the underlying glacial section, sedimentation rates fluctuate around 300-400 cm ka^{-1}.

3.2 General sediment composition

Sediments mainly consist of dark grey or greenish grey mud and diamict. The general geochemical sediment composition is fairly uniform over the length of the core. Silicon makes up for about 27 wt% of the sediment, and Al about 8 wt%. The TOC content (Figure 2) is on average 0.5 wt% and ranges between 0.3 wt% and 0.8 wt% over the whole record. The Si/Al ratio (Figure 3), an indicator for either coarse-grained sediment components or biogenic silica, is stable around 3.3, slightly above the average shale (AS; Wedepohl, 1971) value of 3.1, indicating no consistent enrichments in opal or quartz. The Ca/Al ratio is on average around 0.4, higher than average shale, potentially due to a contribution of biogenic carbonate tests. Average shale does not necessarily provide the most suitable reference composition at this site. Recent research (Penkrot et al., 2018b) has shown that the Chugach-Prince-William-Terrane, which is exposed in the Alaskan Coastal Range (Figure 1a), is the major sediment source to Site U1419. Table 1 shows average element values for the metamorphic rocks of the Chugach Terrane (CT, Barker et al., 1992) in comparison to average shale (Wedepohl,

1971). The K/Al ratio varies between 0.17 and 0.21, and Mg/Al ranges between 0.2 and 0.3. Averages in our samples and AS values for these elements are: K: 1.5 and 2.99 and Mg: 2.1 and 1.57, respectively (data not shown). Hence, Mg exceeds AS values, whereas K falls below AS contents. Values for both elements in our samples are closer to the values of the CT material (Barker et al., 1992).

3.3 Bacteriohopanetetrol lipids

BHT-34*S* is present throughout the sediment record and accounts for between 0.3 and 3.4 mg BHT / g TOC. BHT-*x* ranges from below detection limit to 1.4 mg BHT / g TOC. The ratio between BHT-*x* and total BHT ranges from 0 to 0.6, with an average of 0.23 (Figure 2). The highest ratio occurs at 46.0 cal ka BP (83.31 mbsf). Additional peaks in the BHT-*x*/BHTtot ratio occur at 40.5 cal ka BP (71.28 mbsf), 33.1 cal ka BP (62.38 mbsf), 28.9 cal ka BP (36.51 mbsf) and 19.6 cal ka BP (16.83 mbsf) (Figure 2).

3.4 Inorganic redox proxies

No long-term trends are observable in the TM records (Figure 4). Average contents are 6 wt% Fe, 172 ppm V, 103 ppm Cr, 45 ppm Cu and 45 ppm Ni and. Iron, Cr and V are slightly above the AS values (i.e., 4.8 wt% Fe, 130 ppm V, 90 ppm Cr) but Fe and Cr are below the CT values (i.e., 1 wt% Fe, 163 ppm Cr). Average Cu content in the GOA record is equal to AS (45 ppm) and Ni is lower than AS (68 ppm). Both Cu and Ni are higher than the CT background (38 ppm Cu and 33 ppm Ni).

Element/Al ratios (Figure 5) for the above-mentioned TM are (Average, Min, Max) Fe %/% (0.7, 0.58, 0.82), V ppm/% (19.9, 15.4, 24.3), Cr ppm/% (11.8, 8.7, 14.9), Cu ppm/% (5.2, 3.6, 7.7) and Ni ppm/% (5.2, 3.8, 6.7).

Uranium contents range from 1.5 ppm to 3.1 ppm with an average of 2 ppm. Hence, U lies below AS (3.7 ppm) in all analyzed samples and is close to the CT background (2.1 ppm).

U/Al ratios are (ppm/%): Average: 0.23; Min: 0.17; Max: 0.35; AS: 0.42 and CT: 0.25 (Figure 4).

Molybdenum contents were only analyzed by XRF and are close to quantification limit (detection limit: 1 ppm; quantification limit: 2 ppm). This indicates no significant Mo enrichment in the sediments. Molybdenum ranges from 0 to 3 ppm (Mo/Al –up to 0.4, Average = 0.1) and results for Mo are in discrete 1 ppm steps due to proximity to the XRF quantification limit. In most samples, Mo contents lie below AS (1.3 ppm). No Mo contents are reported from CT (Figure 4).

4. Discussion

4.1 Anammox in the GOA in relation to northern hemispheric paleoclimate

Previous research using anammox in marine sediments is sparse. Jaeschke et al. (2009b) inferred that variations in the concentration of ladderane fatty acids in an Arabian Sea sediment record spanning the last 140 ka was molecular evidence of anammox activity, which increased with enhanced ODZ intensity during interglacials. Additionally, Matys et al. (2017) used the BHT ratio as a proxy for anammox and anoxia in the water column and sediments of the Humboldt Current System, Chile, and Rush et al. (2019) used the BHT-*x* biomarker to reconstruct basin-wide anoxic events in the Mediterranean. Here, the BHT ratio is used as a biomarker for the presence of anammox bacteria, and positive excursions in the ratio are interpreted as oxygen depletion due to increased intensity of the ODZ of the GOA.

Praetorious and Mix (2014) showed that late Pleistocene climatic trends in the GOA generally mirror the climate signals recorded by Greenland ice cores. Therefore, we use NGRIP $\delta^{18}O$ to reveal connections between ODZ fluctuations in the GOA and northern hemispheric climate. Between ~50 and 30 ka BP, northern hemispheric climate, as recorded by the $\delta^{18}O$ signal of the NGRIP ice core, followed a gradual cooling trend (Figure 3). This

trend was interrupted by repeated, several hundred- to thousand-year-long warming and subsequent cooling phases, the Dansgaard/Oeschger Events (D/O Events; Dansgaard et al., 1983; red peaks in NGRIP $\delta^{18}O$ record in Figure 3). After ~30 ka BP, global climate warmed until ~17 ka BP. This warming episode was also interrupted by shorter and less extreme D/O Events.

Our record of ODZ intensity, inferred from BHT ratio, in the GOA generally follows the global climate trends as represented by NGRIP (Figure 3). Over the investigated period, the highest BHT ratio occurs during a D/O event between 46.7 and 43.7 cal ka BP. Further, smaller peaks of BHT ratio that coincide with warm phases of the NGRIP record occur at 58.8, 38, 35, 32, 28.8 and 19.5 cal ka BP, (Figure 3). There are also BHT ratio peaks that do not correspond to significant peaks in NGRIP $\delta^{18}O$ (e.g., at 41 ka BP) and vice versa (e.g., the NGRIP $\delta^{18}O$ peaks at 17, 23.3 32.5 and 33.3 cal ka BP do not correspond to peaks in the BHT ratio). The latter may, however, be partly due to the lower sample resolution, which might not catch narrow peaks of BHT. The overall picture is that anammox, and thus oxygen limited conditions, prevailed throughout the past 60 ka and the degree of oxygen deficiency in the GOA water column at Site U1419 was closely aligned with northern hemispheric climate over the last glacial period, consistent with records for the last deglacial in the GOA (McKay et al., 2005; Barron et al., 2009; Addison et al., 2012) and the wider North Pacific area (Cannariato and Kennett, 1999; Zheng et al., 2000; Cartapanis et al., 2011).

The observed climate-ODZ relationship could have been caused by changes in organic matter production and deposition, and/or a rearrangement of ocean currents (McKay et al., 2005). The general TOC content over the record of Site U1419 is consistently below 1 wt% and thus much lower than TOC contents reported in other ODZ sediments. Jaeschke et al. (2009b) for example reported 4 - 6 wt% TOC for the ODZ of the Arabian Sea. In the GOA; however, high sedimentation rates (> 200 cm ka^{-1}) caused by high rates of glacial erosion of lithogenic

material might have efficiently diluted the sedimentary TOC content. As TOC content and TOC/Al ratio do not systematically increase in intervals with higher BHT ratios at Site U1419 (Figure 3), there is no support for enhanced organic matter deposition or preservation during intervals with a more intense ODZ (as indicated by the BHT ratio). However, the TOC record could have been overprinted by early diagenetic degradation of organic matter, so-called burndown. Due to this bias in the TOC record, we aim to evaluate if warmer climatic conditions in the GOA could have facilitated higher organic matter deposition. Davies et al. (2011) and Addison et al. (2012) suggested that organic matter input from land to the GOA increased during warmer conditions of the last deglaciation. This combined with an elevated input of nutrients (i.e. Fe) due to rising sea levels subsequently enhanced marine primary productivity (Davies et al., 2011; Addison et al., 2012). However, this process probably did not have influence during minor sea-level fluctuations related to D/O Events, as the continental margins along the GOA likely remained fully glaciated (Montelli et al., 2017). Under D/O conditions, melting glaciers could have introduced Fe into the GOA, sustaining marine phytoplankton blooms (Raiswell et al., 2006; Statham et al., 2008). The Fe/Al values of up to 0.8 at Site U1419 during these D/O events support this possibility. Iron is enriched over AS, and even stronger over the CT, in nearly every sample. Davies et al. (2011) and Praetorius et al. (2015) suggested that such hypoxic conditions could have led to further release of Fe^{2+} from suboxic surface sediments where the ODZ impinged on the continental margin. At Site U1419, we find that proxies indicating increased bioproductivity (Si/Al and Ca/Al, Figure 3) follow some trends in the BHT-*x*/BHTtot ratio between 40 and 35 cal ka BP but do not show systematic enrichments. TOC content is not significantly different in the respective intervals from the rest of the core (Figures 2 and 3). We therefore cannot determine if oxygen limitation in the GOA was primarily caused by enhanced remineralization of sinking organic particles produced in surface waters or by limited re-

supply of oxygen to the mid-water masses through stronger thermohaline stratification. The latter would be consistent with Cartapanis et al. (2011, 2012) who proposed a re-organization of global ocean circulation and teleconnections, as well as changes in North Pacific stratification due to freshwater input, during abrupt ice sheet melting/calving events. Accordingly, the GOA was part of a much wider, potentially global, perturbation/reorganization of ocean circulation with widespread stratification along continental margins.

4.2 ODZ behavior recorded by redox sensitive trace metals

To complement our BHT-*x* record of oxygen deficiency within the GOA water column, we analyzed a range of TM that are well-established inorganic proxies for ODZ intensity and bottom water redox conditions (reviews by Brumsack, 2006; Tribovillard et al., 2006). However, no good match between the BHT-*x*/BHTtot ratio and any of the TM records, and consequently between NGRIP $\delta^{18}O$ and TM, is observed (Figure 4).

Two of the most commonly used TM for paleo-redox reconstructions are Mo and U. Uranium is not significantly enriched over the whole record. In fact, with an average of 2 ppm and a maximum of 3.1 ppm, it is below AS (3.7 ppm) in all samples studied and below the CT background (2.1 ppm) in most samples. The samples in which U exceeds the CT background do not, in most cases, show a significant peak in the BHT ratio. For comparison of our Mo and U records with other North Pacific margin sites, McKay et al. (2005) reported enrichments of up to 5.8 ppm for U in sediments deposited under anoxic conditions off Vancouver Island. In modern sediments of the ODZ in the Arabian Sea, U enrichments exceed 12 ppm (Sirocko et al., 2000). Van der Weijden et al. (2006) reported U/Al ratios exceeding 2 ppm/% from the ODZ in the Arabian Sea, and Acharya et al. (2015) concluded that average U contents of 4.1 ppm still indicate an oxic depositional environment.

The apparent discrepancy between our biomarker and TM records in terms of water column redox reconstruction is most likely related to the fundamental processes that lead to TM enrichments in oxygen-depleted sediments. Uranium exists as U(VI) in oxic seawater and is reduced to U(IV) in nitrogenous (= suboxic) waters. Uranium(IV) is less soluble than U(VI) and precipitates from the dissolved into the solid phases. In oxic bottom waters, this reduction process happens within the nitrogenous (suboxic) parts of the sediment, and U is provided through diffusion across the sediment-water interface (Klinkhammer and Palmer, 1991). Under the high sedimentation rates at Site U1419, authigenic U accumulation in the sediment could have been diluted by the input of large amounts of detrital material. Higher detrital sedimentation rates can therefore mask authigenic U accumulations so that no significant sedimentary enrichment is recorded, even below an anoxic water column (Klinkhammer and Palmer, 1991; Liu and Algeo, 2020).

Sedimentation rates at Site U1419 are exceptionally high, nearly constantly exceeding 200 cm ka^{-1}, and episodically exceeding 1000 cm ka^{-1} (Figure 6), translating into mass accumulation rates (MAR) between 50 and 3700 g cm^{-2} ka^{-1} for the studied time period. For comparison, other sites in the ODZ in the Arabian Sea with higher U contents have an order of magnitude lower sedimentation rates (17 cm ka^{-1}, Acharya et al., 2015) and mass accumulation rates (<20 g cm^{-2} ka^{-1}, van der Weijden et al., 2006). These data support the conclusion that very high sedimentation rates indeed control the degree of sedimentary TM accumulations even though they are buried under sub- to anoxic bottom water conditions.

This concept can be further tested by a simple "back-of-the-envelope" calculation. Using numbers from McManus et al. (2005), who calculated U removal to be 2.0 10^{-10} moles cm^{-2} a^{-1} for an exemplary environment within the ODZ at the California Margin, we derive that average mass accumulation rates of ~400 g cm^{-2} ka^{-1} at Site U1419 would only allow for an almost negligible response in sedimentary U contents (estimated at 0.119 ppm), supporting

the notion that sedimentary U accumulation is not significant in high sedimentation rate settings.

The mass accumulation rate of U also follows the profile of the sedimentation rate at Site U1419 (Figure 6). This similarity, and the fact that average U contents match the composition of the CT background, indicates that the bulk U content in the sediments of Site U1419 has a terrigenous source without any significant authigenic component.

Molybdenum has not been analyzed at a sufficient depth resolution to match its pattern directly to the anammox record or the NGRIP $\delta^{18}O$ record. However, its content is close to the XRF quantification limit over the whole record and below AS values (Wedepohl, 1971) in most samples, implying no significant enrichment due to water column euxinia. In contrast to U, Mo is traditionally associated with enrichment in sediments under sulfidic conditions where it reacts with H_2S to form Mo-S species (Helz et al., 1996; Erickson and Helz, 2000) or is incorporated into authigenic pyrite (Morse and Luther, 1999). These processes are controlled by the availability of H_2S, which is produced by bacterial sulfate reduction. Anammox has been observed in sub- to anoxic but non-sulfidic waters (Jensen et al., 2008). Therefore, substantial Mo enrichments due to a sulfidic water column would not be expected at Site U1419. It should be noted, however, that the influence of H_2S on anammox bacteria is not conclusively constrained (Dalsgaard et al., 2014; Lipsewers et al., 2016). Michiels et al. (2019) report anammox activity under H_2S concentrations up to 2.5 µM. Recent research has shown that Mo can also be enriched in marine sediments under nitrogenous conditions, frequently occurring in ODZs (Scholz et al., 2017, Tessin et al., 2018). In these studies, enrichment is caused by adsorption onto Fe(oxyhydr)oxides which are precipitated from Fe^{2+} that is diffusing back into the water column and re-oxidized with nitrate as terminal electron acceptor – a plausible process in the GOA (see discussion on Fe cycling above). In the ODZ off Peru, significant enrichments of sedimentary Mo have been reported despite non-sulfidic

bottom water conditions (Scholz et al., 2017). Similar to U, at Site U1419, higher sedimentation rates would also attenuate sedimentary enrichment of Mo because the enrichment via Fe shuttling will be masked by high detrital deposition rates. Potentially, even efficient Fe shuttling out of the sediments is prevented by the high background accumulation rates.

While neither U nor Mo show significant enrichments at Site U1419, the element/Al ratios of Cr, Cu, Ni and V show some similarities to the BHT ratio (Figure 5). Still, these relationships are neither systematic nor constant throughout the record. The BHT ratio only matches Cr and V between 38 and 17 cal ka BP, and Cu and Ni between 40 and 30 cal ka BP. The overall inconsistency between TM and the NGRIP $\delta^{18}O$ record would appear to suggest the persistent absence of an ODZ at Site U1419 over the studied time period.

The inhibition of TM accumulation by high detrital sedimentation rates described for Mo and U should also prevent the accumulation of Cr, Cu, Ni and V that tend to be enriched in sediments under suboxic to sulfidic conditions (Huerta-Diaz and Morse, 1992; Tribovillard et al., 2006). However, Cr, Cu and V contents at U1419 are on average slightly above AS values (Wedepohl, 1971), and only Ni is depleted. In comparison to the CT background material, Cr at Site U1419 is lower while Cu and Ni are slightly higher. Furthermore, the individual accumulation rates for these TM follow trends in sediment accumulation rate and Al content. This indicates that slightly elevated TM contents, as we observe them in our samples, are unrelated to past redox conditions, but instead have significant detrital contributions from lithologies with higher TM contents than the AS composition. Differences in our data from the CT values (Table 1) may arise from sorting processes during transport and deposition or admixture of secondary source materials (Penkrot et al., 2018b) , e.g., from the Orca-Valdez Group in the Prince William Terrane where higher metal concentrations have been reported (Lull and Plafker, 1990). Elevated Mg and lower K contents relative to

AS indicate some mafic contribution to the detrital background (Le Maitre, 1976). Both Mg and K contents are much closer to CT than to AS, supporting this hypothesis. We conclude that any redox-related accumulation of Cr, Cu, Ni and V was prevented at U1419 by high background sedimentation rates (as for Mo and U), but that this background material had slightly elevated Cr and potentially V contents (V not reported in Barker et al., 1992) that were imprinted onto the newly deposited sediments.

Copper and Ni, which are both enriched in our sediment samples relative to the CT material, also play a role as micronutrients during primary production (Boyle et al., 1977; Böning et al., 2015; Steiner et al., 2017) and are removed from the water column by organic matter deposition. Hence, they can also be affected by changes in bioproductivity (Nameroff et al., 2002). In our samples, however, Cu and Ni do not show an observable relationship with TOC. The Ni depletion relative to AS is another indicator that deoxygenation was probably not driven by enhanced TOC export to the seafloor.

Manganese concentrations are often complementary used as a proxy for oxic conditions. Mn-oxides form in the presence of oxygen and accumulate above average crustal concentrations under oxic water columns. In oxygen-depleted conditions Mn-oxides are reduced and dissolved Mn^{2+} diffuses out of the seafloor (Calvert and Pedersen, 2007). At Site U1419, Mn concentrations (Table 1) and Mn/Al values (data not shown) are in the range of AS and CT. They show very low down core variability. This is a further indication that high sedimentation rates neither allow for significant precipitational enrichment or diffusive depletion due to redox conditions.

Overall, our data show an apparent discrepancy between BHT-*x* biomarker and TM records at Site U1419 in terms of interpreting bottom water redox conditions. The BHT ratio follows the NGRIP $\delta^{18}O$ record, and both follow dissolved oxygenation patterns reported by other

studies for the North Pacific and GOA during the last deglaciation (i.e., general warming leads to an intensification of the ODZ; Cannariato and Kennett, 1999; Cartapanis et al., 2011). We conclude that the BHT-*x* biomarker indeed records the intensity of the ODZ at Site U1419, whereas the redox-sensitive TM records are unreliable at high sedimentation rates. Settings with high sedimentation rates such as Site U1419, or variations in the geochemical composition of the detrital input, can lead to TM records that are unreliable for paleo-redox reconstructions (Tribovillard et al., 2006; Steiner et al., 2017). A recent study (Belanger et al., 2020) which focuses on the Deglacial and Holocene intervals (< 22 ka BP) of Site U1419 found co-variations of U/Al and Mo/Al with foraminifera faunal assemblages indicative of suboxic to anoxic conditions. The overall reported TM concentrations are, however, on the same order of magnitude as presented in this study, supporting the assumption that high sedimentation rates potentially mask the signal of redox sensitive TM accumulation.

With the average removal of U at 2.0 10^{-1} nmol cm^{-2} a^{-1} reported by Klinkhammer and Palmer (1991), we derive that a U enrichment of more than 1 ppm is only possible under sediment accumulation rates < 50 g cm^{-2} ka^{-1}.

An additional factor affecting TM concentrations could be the seasonality of the GOA ODZ. Recently, Bennett and Canfield (2020) showed that seasonal ODZs exhibit TM accumulations closer to oxic environments than to perennial ODZs. This might be a further indication, that the BHT ratio is a better suited proxy in environments where redox sensitive TM fail to provide unequivocal paleo-redox records.

5. Conclusion

We examined sediment samples from Site U1419 in the Gulf of Alaska spanning the period between ~60 and 15 cal ka BP using the new BHT-*x* biomarker to reconstruct anammox activity and ODZ intensity. We compare BHT-*x* results to redox-sensitive trace metal records.

The anammox biomarker record varied in phase with northern hemispheric climate as recorded by the NGRIP ice cores, supporting that northern hemispheric climate drove the extent and/or intensity of the ODZ in the GOA over the past ~60 ka. This is consistent with previous studies across the North Pacific over the past ~17 ka. The ODZ became more intense during warmer periods and less intense during colder ones. Unlike the biomarker records, redox sensitive TMs do not indicate the presence of an ODZ over the study period. Trace metal accumulation is minor compared to other sites in the North Pacific and in the Arabian Sea ODZ, and does not follow any clear trend. We postulate that the exceptionally high sedimentation rates at Site U1419 (episodically exceeding ~1000 cm ka^{-1}) prevented the diffusion of U into the sediments and diluted any enrichments of Cu, Mo and Ni in authigenic phases.

6. Acknowledgements

The authors sincerely thank the Captain, Crew, and Scientific Party of the R/V Joides Resolution for the realization of IODP Expedition 341. We also thank Rachel Schwarz-Narbonne for insightful discussions about the BHT biomarker. Further thanks go to Alexandra Crawford (Newcastle), Phillip Green (Newcastle), as well as Carola Lehners and Eleonore Gründken (Oldenburg) for supporting the analytical work. This research was funded by the Natural Environment Research Council (NERC), the European Consortium for Ocean Research Drilling (ECORD), UK IODP, the School of Civil Engineering and Geosciences at Newcastle University and NSF award ### to Dr. Jaeger. Additional funding came from NERC project ANAMMARKS (NE/N011112/1) awarded to Dr. Rush. Dr. Rush also receives funding from the Soehngen Institute for Anaerobic Microbiology (SIAM) though a gravitation grant (024.002.002) from the Dutch ministry for Education, Culture and Science.

Data Availability

Supplementary data to this article can be found online at #####

Literature

Acharya, S.S., Panigrahi, M.K., Gupta, A.K., Tripathy, S., 2015. Response of trace metal redox proxies in continental shelf environment: The Eastern Arabian Sea scenario. Continental Shelf Research 106, 70-84. https://doi.org/10.1016/j.csr.2015.07.008

Addison, J.A., Finney, B.P., Dean, W.E., Davies, M.H., Mix, A.C., Stoner, J.S., Jaeger, J.M., 2012. Productivity and sedimentary δ15N variability for the last 17,000 years along the northern Gulf of Alaska continental slope. Paleoceanography 27. https://doi.org/10.1029/2011PA002161

Barker, F., Farmer, G.L., Ayuso, R.A., Plafker, G., Lull, J.S., 1992. Melting in an Accretionary Prism in the Forearc. Journal of Geophysical Research 97, 6757–6778. https://doi.org/10.1029/92JB00257

Barron, J.A., Bukry, D., Dean, W.E., Addison, J.A., Finney, B., 2009. Paleoceanography of the Gulf of Alaska during the past 15,000 years: results from diatoms, silicoflagellates, and geochemistry. Marine Micropaleontology 72, 176-195. https://doi.org/10.1016/j.marmicro.2009.04.006

Belanger, C. L., Du, J., Payne, C. R., Mix, A. C., 2020. North Pacific deep-sea ecosystem responses reflect post-glacial switch to pulsed export productivity, deoxygenation, and destratification. Deep Sea Research Part I: Oceanographic Research Papers, 103341. https://doi.org/10.1016/j.dsr.2020.103341.

Bennett, W. W., Canfield, D. E., 2020. Redox-sensitive trace metals as paleoredox proxies: A review and analysis of data from modern sediments. Earth-Science Reviews, 103175. https://doi.org/10.1016/j.earscirev.2020.103175.

Berndmeyer, C., Thiel, V., Schmale, O., Blumenberg, M., 2013. Biomarkers for aerobic methanotrophy in the water column of the stratified Gotland Deep (Baltic Sea). Organic geochemistry 55, 103-111. https://doi.org/10.1016/j.orggeochem.2012.11.010

Bernhard, J.M., Reimers, C.E., 1991. Benthic foraminiferal population fluctuations related to anoxia: Santa Barbara Basin. Biogeochemistry 15, 127-149. https://doi.org/10.1007/BF00003221

Bligh, E.G., Dyer, W.J., 1959. A rapid method of total lipid extraction and purification. Canadian journal of biochemistry and physiology 37, 911-917. https://doi.org/10.1139/y59-099

Böning, P., Shaw, T., Pahnke, K., Brumsack, H.-J., 2015. Nickel as indicator of fresh organic matter in upwelling sediments. Geochimica et Cosmochimica Acta 162, 99-108. https://doi.org/10.1016/j.gca.2015.04.027

Boyle, E.A., Sclater, F.R., Edmond, J.M., 1977. The distribution of dissolved copper in the Pacific. Earth and planetary science letters 37, 38-54. https://doi.org/10.1016/0012-821X(77)90144-3

Breitburg, D., Levin, L.A., Oschlies, A., Grégoire, M., Chavez, F.P., Conley, D.J., Garçon, V., Gilbert, D., Gutiérrez, D., Isensee, K., Jacinto, G.S., Limburg, K.E., Montes, I., Naqvi, S.W.A., Pitcher, G.C., Rabalais, N.N., Roman, M.R., Rose, K.A., Seibel, B.A., Telszewski, M., Yasuhara, M., Zhang, J., 2018. Declining oxygen in the global ocean and coastal waters. Science (80-.). https://doi.org/10.1126/science.aam7240

Bristow, L.A., Dalsgaard, T., Tiano, L., Mills, D.B., Bertagnolli, A.D., Wright, J.J., Hallam, S.J., Ulloa, O., Canfield, D.E., Revsbech, N.P., Thamdrup, B., 2016. Ammonium and nitrite oxidation at nanomolar oxygen concentrations in oxygen minimum zone waters. Proceedings of the National Academy of Sciences 113, 10601-10606. https://doi.org/10.1073/pnas.1600359113.

Brumsack, H.J., 2006. The trace metal content of recent organic carbon-rich sediments: Implications for Cretaceous black shale formation. Palaeogeography Palaeoclimatology Palaeoecology https://doi.org/10.1016/j.palaeo.2005.05.011

Burdige, D.J., 2007. Preservation of organic matter in marine sediments: Controls, mechanisms, and an imbalance in sediment organic carbon budgets? Chemical Reviews 107, 467–485.

https://doi.org/10.1021/cr050347q

Calvert, S.E., Pedersen, T.F., 2007. Chapter fourteen elemental proxies for palaeoclimatic and palaeoceanographic variability in marine sediments: interpretation and application. Developments in Marine Geology 1, 567-644. https://doi.org/10.1016/S1572-5480(07)01019-6

Cannariato, K.G., Kennett, J.P., 1999. Climatically related millennial-scale fluctuations in strength of California margin oxygen-minimum zone during the past 60 ky. Geology 27, 975-978. https://doi.org/10.1130/0091-7613(1999)027<0975:CRMSFI>2.3.CO;2

Cartapanis, O., Tachikawa, K., Romero, O.E., Bard, E., 2014. Persistent millennial-scale link between Greenland climate and northern Pacific Oxygen Minimum Zone under interglacial conditions. Climate of the Past 10, 405. https://doi.org/10.5194/cp-10-405-2014

Cartapanis, O., Tachikawa, K., Bard, E., 2012. Latitudinal variations in intermediate depth ventilation and biological production over northeastern Pacific Oxygen Minimum Zones during the last 60 ka. Quaternary Science Reviews 53, 24-38. https://doi.org/10.1016/j.quascirev.2012.08.009

Cartapanis, O., Tachikawa, K., Bard, E., 2011. Northeastern Pacific oxygen minimum zone variability over the past 70 kyr: Impact of biological production and oceanic ventilation. Paleoceanography 26. https://doi.org/10.1029/2011PA002126

Clark, P.U., Dyke, A.S., Shakun, J.D., Carlson, A.E., Clark, J., Wohlfarth, B., Mitrovica, J.X., Hostetler, S.W., McCabe, A.M., 2009. The last glacial maximum. Science 325, 710-714. https://doi.org/10.1126/science.1172873

Codispoti, L.A., Brandes, J.A., Christensen, J.P., Devol, A.H., Naqvi, S.W.A., Paerl, H.W., Yoshinari, T., 2001. The oceanic fixed nitrogen and nitrous oxide budgets: Moving targets as we enter the anthropocene? Scientia Marina 65, 85-105. https://doi.org/10.3989/scimar.2001.65s285

Cooke, M.P., van Dongen, B.E., Talbot, H.M., Semiletov, I., Shakhova, N., Guo, L., Gustafsson, Ö., 2009. Bacteriohopanepolyol biomarker composition of organic matter exported to the Arctic Ocean by seven of the major Arctic rivers. Organic Geochemistry 40, 1151-1159. https://doi.org/10.1016/j.orggeochem.2009.07.014

Dalsgaard, T., Stewart, F.J., Thamdrup, B., De Brabandere, L., Revsbech, N.P., Ulloa, O., Canfield, D.E., DeLong, E.F., 2014. Oxygen at nanomolar levels reversibly suppresses process rates and gene expression in anammox and denitrification in the oxygen minimum zone off northern Chile. MBio 5, e01966-01914. https://doi.org/10.1128/mBio.01966-14

Dansgaard, W., Oeschger, H., Langway, C.C., 1983. ICE Core Indications of Abrupt Climatic Changes, Palaeoclimatic Research and Models. Springer, pp. 72-73. https://doi.org/10.1007/978-94-009-7236-0_9

Davies, M.H., Mix, A.C., Stoner, J.S., Addison, J.A., Jaeger, J., Finney, B., Wiest, J., 2011. The deglacial transition on the southeastern Alaska Margin: Meltwater input, sea level rise, marine productivity, and sedimentary anoxia. Paleoceanography 26. https://doi.org/10.1029/2010PA002051

Devol, A.H., Hartnett, H.E., 2001. Role of the oxygen-deficient zone in transfer of organic carbon to the deep ocean. Limnology and Oceanography 46, 1684–1690. https://doi.org/10.4319/lo.2001.46.7.1684

Emery, K.O., Hülsemann, J., 1961. The relationships of sediments, life and water in a marine basin. Deep Sea Research, 8, 165-IN2. https://doi.org/10.1016/0146-6313(61)90019-3

Erickson, B.E., Helz, G.R., 2000. Molybdenum (VI) speciation in sulfidic waters:: stability and lability of thiomolybdates. Geochimica et Cosmochimica Acta 64, 1149-1158. https://doi.org/10.1016/S0016-7037(99)00423-8

Gilly, W.F., Beman, J.M., Litvin, S.Y., Robison, B.H., 2013. Oceanographic and Biological Effects of Shoaling of the Oxygen Minimum Zone. Annual Reviews in Marine Science 5, 393–420. https://doi.org/10.1146/annurev-marine-120710-100849

Hamersley, M.R., Lavik, G., Woebken, D., Rattray, J.E., Lam, P., Hopmans, E.C., Damsté, J.S.S., Krüger, S., Graco, M., Gutiérrez, D., 2007. Anaerobic ammonium oxidation in the Peruvian oxygen minimum zone. Limnology and Oceanography 52, 923-933. https://doi.org/10.4319/lo.2007.52.3.0923

Hartnett, H., Keil, R., Hedges, J., Devol, A., 1998. Influence of oxygen exposure time on organic

carbon preservation in continental margin sediments. Nature 391, 572–575. https://doi.org/10.1038/35351

Haslett, J., Parnell, A., 2008. A simple monotone process with application to radiocarbon-dated depth chronologies. Journal of the Royal Statistical Society: Series C (Applied Statistics), 57: 399-418. https://doi.org/10.1111/j.1467-9876.2008.00623.x

Hedges, J.I., Keil, R.G., 1995. Sedimentary organic matter preservation: an assessment and speculative synthesis. Marine Chemistry, 49, 81–115. https://doi.org/10.1016/0304-4203(95)00008-F

Helz, G.R., Miller, C.V., Charnock, J.M., Mosselmans, J.F.W., Pattrick, R.A.D., Garner, C.D., Vaughan, D.J., 1996. Mechanism of molybdenum removal from the sea and its concentration in black shales: EXAFS evidence. Geochimica et Cosmochimica Acta 60, 3631-3642. https://doi.org/10.1016/0016-7037(96)00195-0

Huerta-Diaz, M.A., Morse, J.W., 1992. Pyritization of trace metals in anoxic marine sediments. Geochimica et Cosmochimica Acta 56, 2681-2702. https://doi.org/10.1016/0016-7037(92)90353-K

Jaeger, J.M., Gulick, S.P.S., LeVay, L.J., Asahi, H., Bahlburg, H., Belanger, C.L., Berbel, G.B.B., Childress, L.B., Cowan, E.A., Drab, L., 2014. Proceedings of the Integrated Ocean Drilling Program Vol. 341: Expedition reports Southern Alaska margin. Integrated Ocean Drilling Program.

Jaeschke, A., Rooks, C., Trimmer, M., Nicholls, J.C., Hopmans, E.C., Schouten, S., Damsté, J.S.S., 2009a. Comparison of ladderane phospholipid and core lipids as indicators for anaerobic ammonium oxidation (anammox) in marine sediments. Geochimica et Cosmochimica Acta 73, 2077-2088. https://doi.org/10.1016/j.gca.2009.01.013

Jaeschke, A., Ziegler, M., Hopmans, E.C., Reichart, G.J., Lourens, L.J., Schouten, S., Sinninghe Damsté, J.S., 2009b. Molecular fossil evidence for anaerobic ammonium oxidation in the Arabian Sea over the last glacial cycle. Paleoceanography 24. https://doi.org/10.1029/2008PA001612

Jensen, M.M., Kuypers, M.M.M., Lavik, G., Thamdrup, B., 2008. Rates and regulation of anaerobic ammonium oxidation and denitrification in the Black Sea. Limnology and Oceanography. https://doi.org/10.4319/lo.2008.53.1.0923

Kalvelage, T., Jensen, M.M., Contreras, S., Revsbech, N.P., Lam, P., Günter, M., LaRoche, J., Lavik, G., Kuypers, M.M.M., 2011. Oxygen Sensitivity of Anammox and Coupled N-Cycle Processes in Oxygen Minimum Zones. PLoS ONE 6, e29299-12. https://doi.org/10.1371/journal.pone.0029299.

Kamenov, G.D., Brenner, M., and Tucker, J.L., 2009, Anthropogenic versus natural control on trace element and Sr-Nd-Pb isotope stratigraphy in peat sediments of southeast Florida (USA), ~1500 AD to present: Geochimica et Cosmochimica Acta, v. 73, p. 3549–3567. https://doi.org/10.1016/j.gca.2009.03.017.

Klinkhammer, G.P., Palmer, M.R., 1991. Uranium in the oceans: where it goes and why. Geochimica et Cosmochimica Acta 55, 1799-1806. https://doi.org/10.1016/0016-7037(91)90024-Y

Kusch, S., Walter, S.R.S., Hemingway, J.D., Pearson, A., 2018. Improved chromatography reveals multiple new bacteriohopanepolyol isomers in marine sediments. Organic Geochemistry 124, 12-21. https://doi.org/10.1016/j.orggeochem.2018.07.010.

Kuypers, M.M.M., Sliekers, A.O., Lavik, G., Schmid, M., Jørgensen, B.B., Kuenen, J.G., Damsté, J.S.S., Strous, M., Jetten, M.S.M., 2003. Anaerobic ammonium oxidation by anammox bacteria in the Black Sea. Nature 422, 608-611. https://doi.org/10.1038/nature01472

Lam, P., Kuypers, M.M.M., 2011. Microbial nitrogen cycling processes in oxygen minimum zones. Annual review of marine science 3, 317-345. https://doi.org/10.1146/annurev-marine-120709-142814

Le Maitre, R.W., 1976. The chemical variability of some common igneous rocks. Journal of petrology 17, 589-598. https://doi.org/10.1093/petrology/17.4.589

Lengger, S.K., Rush, D., Mayser, J.P., Blewett, J., Schwartz-Narbonne, R., Talbot, H.M., Middelburg, J.J., Jetten, M.S.M., Schouten, S., Sinninghe Damsté, J.S., Pancost, R.D., 2019. Dark carbon fixation in the Arabian Sea oxygen minimum zone contributes to sedimentary organic carbon (SOM). Global Biogeochemical Cycles. https://doi.org/10.1029/2019GB006282

Lipsewers, Y.A., Hopmans, E.C., Meysman, F.J.R., Damsté, J.S.S., Villanueva, L., 2016. Abundance and diversity of denitrifying and anammox bacteria in seasonally hypoxic and sulfidic sediments of the saline Lake Grevelingen. Frontiers in microbiology 7. https://doi.org/10.3389/fmicb.2016.01661

Lisiecki, L.E., Raymo, M.E., 2005. A Pliocene-Pleistocene stack of 57 globally distributed benthic δ18O records. Paleoceanography 20. https://doi.org/10.1029/2004PA001071

Liu, J., Algeo, T.J., 2020. Beyond redox: control of trace-metal enrichment in anoxic marine facies by watermass chemistry and sedimentation rate, Geochimica et Cosmochimica Acta. https://doi.org/10.1016/j.gca.2020.02.037

Lull, J. S., Plafker, G., 1990. Geochemistry and paleotectonic implications of metabasaltic rocks in the Valdez Group, southern Alaska. *US Geological Survey Bulletin*, *1946*, 29-38.

Matys, E.D., Sepúlveda, J., Pantoja, S., Lange, C.B., Caniupán, M., Lamy, F., Summons, R.E., 2017. Bacteriohopanepolyols along redox gradients in the Humboldt Current System off northern Chile. Geobiology 15, 844-857. https://doi.org/10.1111/gbi.12250

McKay, J.L., Pedersen, T.F., Southon, J., 2005. Intensification of the oxygen minimum zone in the northeast Pacific off Vancouver Island during the last deglaciation: Ventilation and/or export production? Paleoceanography 20. https://doi.org/10.1029/2005PA000979

Michiels, C.C., Huggins, J.A., Giesbrecht, K.E., Spence, J.S., Simister, R.L., Varela, D.E., Hallam, S.J., Crowe, S.A., 2019. Rates and pathways of N2 production in a persistently anoxic fjord: Saanich Inlet, British Columbia. FMARS 6, 4897. https://doi.org/10.3389/fmars.2019.00027.

Moffitt, S.E., Moffitt, R.A., Sauthoff, W., Davis, C.V., Hewett, K., Hill, T.M., 2015. Paleoceanographic insights on recent oxygen minimum zone expansion: Lessons for modern oceanography. PloS one 10, e0115246. https://doi.org/10.1371/journal.pone.0115246

Montelli, A., Gulick, S.P.S., Worthington, L.L., Mix, A., Davies-Walczak, M., Zellers, S.D., Jaeger, J.M., 2017. Late Quaternary glacial dynamics and sedimentation variability in the Bering Trough, Gulf of Alaska. Geology 45, 251-254. https://doi.org/10.1130/G38836.1

Morse, J.W., Luther, G.W., 1999. Chemical influences on trace metal-sulfide interactions in anoxic sediments. Geochimica et Cosmochimica Acta 63, 3373-3378. https://doi.org/10.1016/S0016-7037(99)00258-6

Mulder, A., Van de Graaf, A.A., Robertson, L.A., Kuenen, J.G., 1995. Anaerobic ammonium oxidation discovered in a denitrifying fluidized bed reactor. FEMS microbiology ecology 16, 177-183. https://doi.org/10.1111/j.1574-6941.1995.tb00281.x

Nakakuni, M., Dairiki, C., Kaur, G., Yamamoto, S., 2017. Stanol to sterol ratios in late Quaternary sediments from southern California: An indicator for continuous variability of the oxygen minimum zone. Organic Geochemistry 111, 126-135. https://doi.org/10.1016/j.orggeochem.2017.06.009

Nameroff, T.J., Balistrieri, L.S., Murray, J.W., 2002. Suboxic trace metal geochemistry in the eastern tropical North Pacific. Geochimica et Cosmochimica Acta 66, 1139-1158. https://doi.org/10.1016/S0016-7037(01)00843-2

Ohkushi, K., Kennett, J.P., Zeleski, C.M., Moffitt, S.E., Hill, T.M., Robert, C., Beaufort, L., Behl, R.J., 2013. Quantified intermediate water oxygenation history of the NE Pacific: A new benthic foraminiferal record from Santa Barbara basin. Paleoceanography 28, 453-467. https://doi.org/10.1002/palo.20043

Ortiz, J.D., O'Connell, S.B., DelViscio, J., Dean, W., Carriquiry, J.D., Marchitto, T., Zheng, Y., Van Geen, A., 2004. Enhanced marine productivity off western North America during warm climate intervals of the past 52 ky. Geology 32, 521-524. https://doi.org/10.1130/G20234.1

Oschlies, A., Schulz, K.G., Riebesell, U., Schmittner, A., 2008. Simulated 21st century's increase in oceanic suboxia by CO2-enhanced biotic carbon export. Global Biogeochemical Cycles 22. https://doi.org/10.1029/2007GB003147

Pachauri, R.K., Allen, M.R., Barros, V.R., Broome, J., Cramer, W., Christ, R., Church, J.A., Clarke, L., Dahe, Q., Dasgupta, P., 2014. Climate change 2014: synthesis report. Contribution of Working Groups I, II and III to the fifth assessment report of the Intergovernmental Panel on Climate Change. IPCC.

Paulmier, A., Ruiz-Pino, D., 2009. Oxygen minimum zones (OMZs) in the modern ocean. Progress in

Oceanography 80, 113-128. https://doi.org/10.1016/j.pocean.2008.08.001

Pearson, A., McNichol, A.P., Benitez-Nelson, B.C., Hayes, J.M., Eglinton, T.I., 2001. Origins of lipid biomarkers in Santa Monica Basin surface sediment: a case study using compound-specific Δ 14 C analysis. Geochimica et Cosmochimica Acta 65, 3123-3137. https://doi.org/10.1016/S0016-7037(01)00657-3

Penkrot, M.L., Jaeger, J.M., Cowan, E.A., St-Onge, G., and LeVay, L., 2018a, Multivariate modeling of glacimarine lithostratigraphy combining scanning XRF, multisensory core properties, and CT imagery: IODP Site U1419: Geosphere, v. 14, no. 4, p. 1–26, https://doi.org/10.1130/GES01635.1.

Penkrot, M.L., Jaeger, J.M., Cowan, E.A., Walczak, M.H., Mix, A.C., LeVay, L.2018b, Tectonic and Climate Influences on Spatial and Temporal Variations of Subglacial Erosion; Bering Glacier, Alaska. American Geophysical Union, Fall Meeting 2018, abstract #C51E-1119

Pitcher, A., Villanueva, L., Hopmans, E.C., Schouten, S., Reichart, G.-J., Damsté, J.S.S., 2011. Niche segregation of ammonia-oxidizing archaea and anammox bacteria in the Arabian Sea oxygen minimum zone. The ISME journal 5, 1896-1904. https://doi.org/10.1038/ismej.2011.60

Praetorius, S.K., Mix, A.C., 2014. Synchronization of North Pacific and Greenland climates preceded abrupt deglacial warming. Science (80-.). 345, 444–448. https://doi.org/10.1126/science.1252000

Praetorius, S.K., Mix, A.C., Walczak, M.H., Wolhowe, M.D., Addison, J.A., Prahl, F.G., 2015. North Pacific deglacial hypoxic events linked to abrupt ocean warming. Nature 527, 362–366. https://doi.org/10.1038/nature15753

Raiswell, R., Tranter, M., Benning, L.G., Siegert, M., De'ath, R., Huybrechts, P., Payne, T., 2006. Contributions from glacially derived sediment to the global iron (oxyhydr) oxide cycle: implications for iron delivery to the oceans. Geochimica et Cosmochimica Acta 70, 2765-2780. https://doi.org/10.1016/j.gca.2005.12.027

Rasmussen, S.O., Bigler, M., Blockley, S.P., Blunier, T., Buchardt, S.L., Clausen, H.B., Cvijanovic, I., Dahl-Jensen, D., Johnsen, S.J., Fischer, H., 2014. A stratigraphic framework for abrupt climatic changes during the Last Glacial period based on three synchronized Greenland ice-core records: refining and extending the INTIMATE event stratigraphy. Quaternary Science Reviews 106, 14-28. https://doi.org/10.1016/j.quascirev.2014.09.007

Reimer, P.J., Bard, E., Bayliss, A., Beck, J.W., Blackwell, P.G., Ramsey, C.B., Buck, C.E., Cheng, H., Edwards, R.L., Friedrich, M., Grootes, P.M., Guilderson, T.P., Haflidason, H., Hajdas, I., Hatté, C., Heaton, T.J., Hoffmann, D.L., Hogg, A.G., Hughen, K.A., Kaiser, K.F., Kromer, B., Manning, S.W., Niu, M., Reimer, R.W., Richards, D.A., Scott, E.M., Southon, J.R., Staff, R.A., Turney, C.S.M., van der Plicht, J., 2013. IntCal13 and Marine13 Radiocarbon Age Calibration Curves 0–50,000 Years cal BP. Radiocarbon. https://doi.org/10.2458/azu_js_rc.55.16947

Rohmer, M., Bouvier-Nave, P., Ourisson, G., 1984. Distribution of hopanoid triterpenes in prokaryotes. Microbiology 130, 1137-1150. https://doi.org/10.1099/00221287-130-5-1137

Rush, D., Talbot, H.M., van der Meer, M.T.J., Hopmans, E.C., Douglas, B., Sinninghe Damsté, J.S., 2019. Biomarker evidence for the occurrence of anaerobic ammonium oxidation in the eastern Mediterranean Sea during Quaternary and Pliocene sapropel formation. Biogeosciences Discussions 1–27. https://doi.org/10.5194/bg-2019-27

Rush, D., Damsté, J.S.S., Poulton, S.W., Thamdrup, B., Garside, A.L., González, J.A., Schouten, S., Jetten, M.S.M., Talbot, H.M., 2014. Anaerobic ammonium-oxidising bacteria: A biological source of the bacteriohopanetetrol stereoisomer in marine sediments. Geochimica et Cosmochimica Acta 140, 50-64. https://doi.org/10.1016/j.gca.2014.05.014

Rush, D., Hopmans, E.C., Wakeham, S.G., Schouten, S., Sinninghe Damsté, J.S., 2012. Occurrence and distribution of ladderane oxidation products in different oceanic regimes. Biogeosciences. https://doi.org/10.5194/bg-9-2407-2012

Sáenz, J.P., Wakeham, S.G., Eglinton, T.I., Summons, R.E., 2011. New constraints on the provenance of hopanoids in the marine geologic record: Bacteriohopanepolyols in marine suboxic and anoxic environments. Organic Geochemitry. https://doi.org/10.1016/j.orggeochem.2011.08.016

Schlitzer, R., 2015. Ocean Data Viev. http://odv.awi.de,2015.

Scholz, F., Siebert, C., Dale, A.W., Frank, M., 2017. Intense molybdenum accumulation in sediments underneath a nitrogenous water column and implications for the reconstruction of paleo-redox conditions based on molybdenum isotopes. Geochimica et Cosmochimica Acta. https://doi.org/10.1016/j.gca.2017.06.048

Schwartz-Narbonne, R., Schaeffer, P., Hopmans, E.C., Schenesse, M., Charlton, A.E Jones, M.D., Sinninghe Damsté, J.S., Farhan Ul Haque, M., Jetten, M.S.M., Lengger, S.K., Murrell, C., Normand, P., Nuijten, G.H.L., Talbot, H.M., Rush, D., 2020. A unique bacteriohopanetetrol stereoisomer of marine anammox, Organic Geochemistry. https://doi.org/10.1016/j.orggeochem.2020.103994

Shaffer, G., Olsen, S.M., Pedersen, J.O.P., 2009. Long-term ocean oxygen depletion in response to carbon dioxide emissions from fossil fuels. Nature Geoscience. https://doi.org/10.1038/ngeo420

Sinninghe Damsté, J.S., Strous, M., Rijpstra, W.I.C., Hopmans, E.C., Geenevasen, J.A.J., Van Duin, A.C.T., Van Niftrik, L.A., Jetten, M.S.M., 2002. Linearly concatenated cyclobutane lipids form a dense bacterial membrane. Nature. https://doi.org/10.1038/nature01128

Sirocko, F., Garbe-Schönberg, D., Devey, C., 2000. Processes controlling trace element geochemistry of Arabian Sea sediments during the last 25,000 years. Global and Planetary Change 26, 217-303. https://doi.org/10.1016/S0921-8181(00)00046-1

Statham, P.J., Skidmore, M., Tranter, M., 2008. Inputs of glacially derived dissolved and colloidal iron to the coastal ocean and implications for primary productivity. Global Biogeochemical Cycles 22. https://doi.org/10.1029/2007GB003106

Steiner, Z., Lazar, B., Torfstein, A., Erez, J., 2017. Testing the utility of geochemical proxies for paleoproductivity in oxic sedimentary marine settings of the Gulf of Aqaba, Red Sea. Chemical Geology. https://doi.org/10.1016/j.chemgeo.2017.10.012

Summons, R.E., Jahnke, L.L., Hope, J.M., Logan, G.A., 1999. 2-Methylhopanoids as biomarkers for cyanobacterial oxygenic photosynthesis. Nature 400, 554-557. https://doi.org/10.1038/23005

Talbot, H.M., Farrimond, P., 2007. Bacterial populations recorded in diverse sedimentary biohopanoid distributions. Organic Geochemistry. https://doi.org/10.1016/j.orggeochem.2007.04.006

Talbot, H.M., Sidgwick, F.R., Bischoff, J., Osborne, K.A., Rush, D., Sherry, A., Spencer-Jones, C.L., 2016. Analysis of non-derivatised bacteriohopanepolyols by ultrahigh-performance liquid chromatography/tandem mass spectrometry. Rapid Communication in Mass Spectrometry. https://doi.org/10.1002/rcm.7696

Talbot, H.M., Rohmer, M., Farrimond, P., 2007. Rapid structural elucidation of composite bacterial hopanoids by atmospheric pressure chemical ionisation liquid chromatography/ion trap mass spectrometry. Rapid Communication in Mass Spectrometry. https://doi.org/10.1002/rcm.2911

Talbot, H.M., Watson, D.F., Murrell, J.C., Carter, J.F., Farrimond, P., 2001. Analysis of intact bacteriohopanepolyols from methanotrophic bacteria by reversed-phase high-performance liquid chromatography–atmospheric pressure chemical ionisation mass spectrometry. Journal of Chromatography A 921, 175-185. https://doi.org/10.1016/S0021-9673(01)00871-8

Tessin, A., Chappaz, A., Hendy, I., Sheldon, N., 2019. Molybdenum speciation as a paleo-redox proxy: A case study from Late Cretaceous Western Interior Seaway black shales. Geology. https://doi.org/10.1130/G45785.1

Tribovillard, N., Algeo, T.J., Lyons, T., Riboulleau, A., 2006. Trace metals as paleoredox and paleoproductivity proxies: an update. Chemical Geology 232, 12-32. https://doi.org/10.1016/j.chemgeo.2006.02.012

Van de Graaf, A.A., Mulder, A., de Bruijn, P., Jetten, M.S., Robertson, L.A., Kuenen, J.G., 1995. Anaerobic oxidation of ammonium is a biologically mediated process. Applied and environmental microbiology 61, 1246-1251.

van der Weijden, C.H., Reichart, G.-J., van Os, B.J.H., 2006. Sedimentary trace element records over the last 200 kyr from within and below the northern Arabian Sea oxygen minimum zone. Marine Geology 231, 69-88. https://doi.org/10.1016/j.margeo.2006.05.013

van Dongen, B.E., Talbot, H.M., Schouten, S., Pearson, P.N., Pancost, R.D., 2006. Well preserved Palaeogene and Cretaceous biomarkers from the Kilwa area, Tanzania. Organic Geochemistry https://doi.org/10.1016/j.orggeochem.2006.01.003

Van Winden, J.F., Talbot, H.M., Kip, N., Reichart, G.-J., Pol, A., McNamara, N.P., Jetten, M.S.M., den Camp, H.J.M.O., Damsté, J.S.S., 2012. Bacteriohopanepolyol signatures as markers for methanotrophic bacteria in peat moss. Geochimica et Cosmochimica Acta 77, 52-61. https://doi.org/10.1016/j.gca.2011.10.026

Walczak, M.H., Mix, A.C., Cowan, E.A., Fallon, S., Fifield, L.K., Alder, J., Du, J., Haley, B., Hobern, T., Padman, J., Praetorius, S.K., Schmittner, A., Stoner, J.S., Zellers, S.D., In Press. Phasing of millennial-scale climate variability in the Pacific and Atlantic Oceans.

Ward, B.B., 2013. How nitrogen is lost. Science 341, 352-353. https://doi.org/10.1126/science.1240314

Wedepohl, K.H., 1971. Environmental influences on the chemical composition of shales and clays. Physics and Chemistry of the Earth 8, 305-333. https://doi.org/10.1016/0079-1946(71)90020-6

Zheng, Y., Geen, A., Anderson, R.F., Gardner, J.V., Dean, W.E., 2000. Intensification of the northeast Pacific oxygen minimum zone during the Bølling-Allerød warm period. Paleoceanography 15, 528-536. https://doi.org/10.1029/1999PA000473

Zhu, C., Talbot, H.M., Wagner, T., Pan, J.-M., Pancost, R.D., 2011. Distribution of hopanoids along a land to sea transect: implications for microbial ecology and the use of hopanoids in environmental studies. Limnology and Oceanography 56, 1850-1865. https://doi.org/10.4319/lo.2011.56.5.1850

Figure 1: A) Bathymetric map of area of investigation, CT indicates approximate position of Chugach Terrane; B) Annually averaged oxygen content (ml L^{-1}) in the Gulf of Alaska (GOA) at 700 m water depth (Site U1419: 721 m); red line A'-B' indicates cross section in panel C; C) Depth position of Site U1419 within the oxygen-deficient zone (ODZ) in the GOA; annually averaged oxygen content (ml L^{-1}). (Map created with Ocean Data view; Schlitzer, 2015; O_2 data from World Ocean Atlas 2005; Garcia et al., 2006).

Figure 2: Concentrations of organic matter and bacteriohopanetetrol at Site U1419: A) TOC as wt% of dry sediment, B) BHT-34*S* and C) BHT-*x* as mg BHT g^{-1} TOC, D) the biomarker ratio used in this study BHT-*x*/BHTtot and the E) sedimentation rate in cm ka^{-1}.

Figure 3: Organic geochemical data and bioproductivity proxies at Site U1419: A) NGRIP $\delta^{18}O$ V-SMOW, B) BHT ratio, C) TOC (wt%), D) Si/Al and E) Ca/Al from this study, $\delta^{18}O$ from NGRIP ice core as reference for northern hemispheric climate from Rasmussen et al.

(2014). Reddish colors indicate warmer periods, bluish/purple colors indicate cooler phases (colors do not correspond to actual temperatures).

Figure 4: Inorganic geochemical data at Site U1419. A) Contents of Fe (wt%) and B - G) trace metals (wt ppm). Dashed black lines indicate average shale content (Wedepohl, 1971) expect for Ni, and U (out of range). Dashed blue lines indicate Chugach Terrane content (Barker et al., 1992) except for Fe (out of range), V and Mo (data not available). Shaded area in A) is BHT ratio for comparison. Light blue graph in A) is NGRIP $\delta^{18}O$ V-SMOW for comparison.

Figure 5: Element/Al ratios at Site U1419. A) Fe (wt%/wt%) and B - G) TM (wt ppm/wt%), Dashed black lines indicate average shale content (Wedepohl, 1971) expect for Ni/Al and U/Al (out of range). Dashed blue lines indicate Chugach Terrane content (Barker et al., 1992) except for Fe/Al, Cr/Al (out of range), V/Al and Mo/Al (data not available). Shaded area in A) is BHT ratio for comparison. Light blue graph in A) is NGRIP $\delta^{18}O$ V-SMOW for comparison.

Figure 6: A) Sedimentation rate (cm ka^{-1}) and B – G) TM mass accumulation rates (mg cm^{-2} ka^{-1}) for minor elements at Site U1419. Shaded area in A) is BHT ratio for comparison. Light blue graph in A) is NGRIP $\delta^{18}O$ V-SMOW for comparison.

Table 1: Average element values for comparison material Average Shale (AS, Wedepohl, 1971; 1991), Chugach Terrane (CT, Barker et al., 1992) and Site U1419.

Element	**Average Shale**	**AS/Al**	**Chugach Terrane**	**CT/Al**	**Average U1419 (± Std. Dev.)**
Si	27.53 %	3.11	31.59 %	3.74	26.85 % (±8.8)

Al	8.84 %	-	8.45 %	-	8.27 % (±0.2)
Fe	4.83 %	0.55	0.97 %	0.11	6.08 % (±0.7)
Ca	1.57 %	0.18	1.45 %	0.17	3.05 % (±0.3)
K	2.99 %	0.34	1.94 %	0.23	1.53 % (±0.1)
Mg	1.57 %	0.18	1.45 %	0.17	2.12 % (±0.2)
Mn	0.09 %	0.01	0.08 %	0.01	0.08 % (±0.01)
Cr	90 ppm	10.18 ppm/%	63 ppm	7.46 ppm/%	103 ppm (±1.1)
Cu	45 ppm	5.09 ppm/%	38 ppm	4.50 ppm/%	45 ppm (±5.9)
Mo	1.3 ppm	0.15 ppm/%	-	-	1.1 ppm (±0.9)
Ni	68 ppm	7.69 ppm/%	33 ppm	3.91 ppm/%	45 ppm (±4.6)
U	3.7 ppm	0.42 ppm/%	2.1 ppm	0.25 ppm/%	2.0 ppm (±0.3)
V	130 ppm	14.71 ppm/%	-	-	172 ppm (±13)

Declaration of interests

x The authors declare that they have no known competing financial interests or personal relationships that could have appeared to influence the work reported in this paper.

☐The authors declare the following financial interests/personal relationships which may be considered as potential competing interests:

Highlights

1) Persistent Oxygen Deficient Zone in the Gulf of Alaska since 60 ka BP
2) ODZ intensifies during warmer paleoclimate events
3) ODZ dynamics recorded by novel BHT-*x* biomarker
4) ODZ dynamics not recorded by redox sensitive trace elements
5) Proxy discrepancy due to dilution by high sedimentation rates

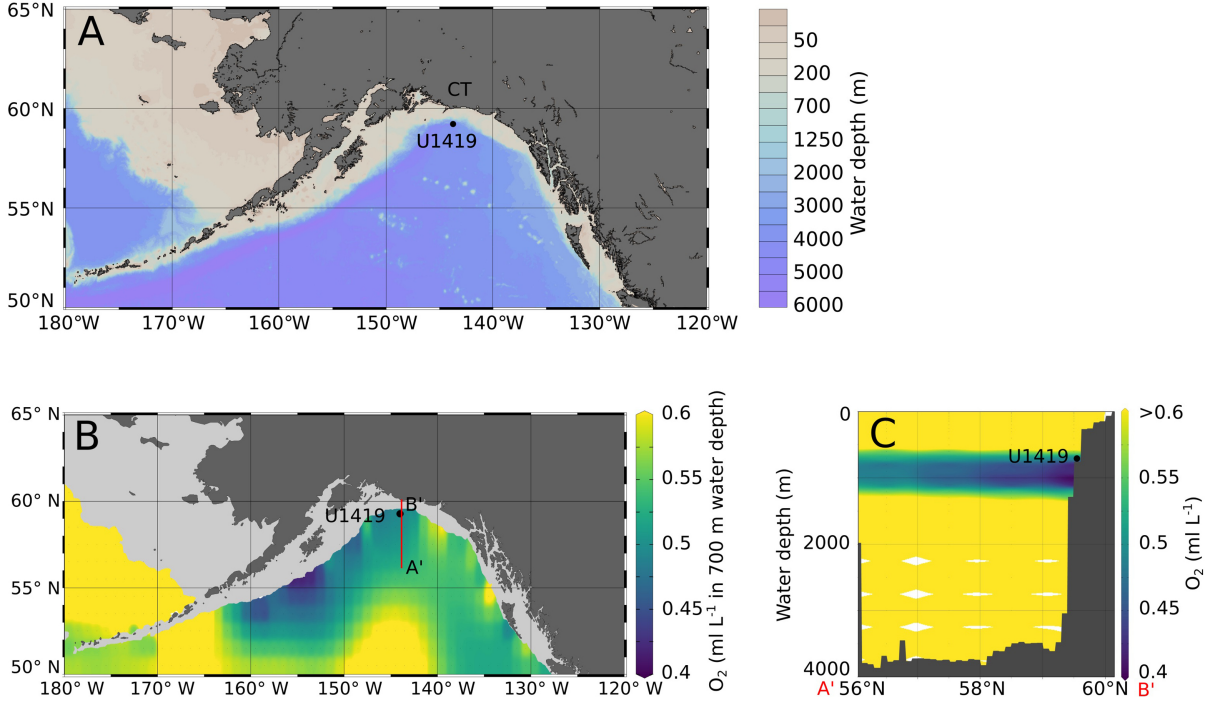
A
CT
U1419
65°N
60°N
55°N
50°N
180°W
170°W
160°W
150°W
140°W
130°W
120°W
Water depth (m)
50
200
700
1250
2000
3000
4000
5000
6000
B
U1419
B'
A'
65° N
60° N
55° N
50° N
180° W
170° W
160° W
150° W
140° W
130° W
120° W
O2 (ml L-1 in 700 m water depth)
0.6
0.55
0.5
0.45
0.4
C
U1419
Water depth (m)
0
2000
4000
A'
56°N
58°N
60°N
B'
>0.6
0.55
0.5
0.45
0.4
O2 (ml L-1)

Figure 1

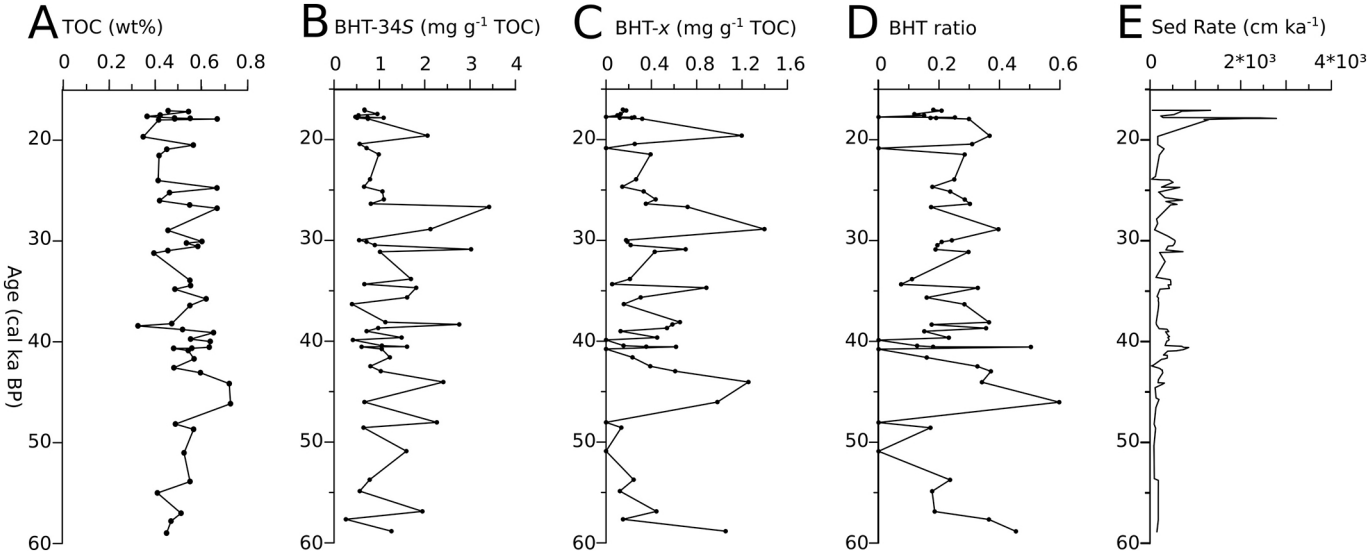
A TOC (wt%)
0 0.2 0.4 0.6 0.8
B BHT-34S (mg g-1 TOC)
0 1 2 3 4
C BHT-x (mg g-1 TOC)
0 0.4 0.8 1.2 1.6
D BHT ratio
0 0.2 0.4 0.6
E Sed Rate (cm ka-1)
0 2*10³ 4*10³
Age (cal ka BP)
20
30
40
50
60

Figure 2

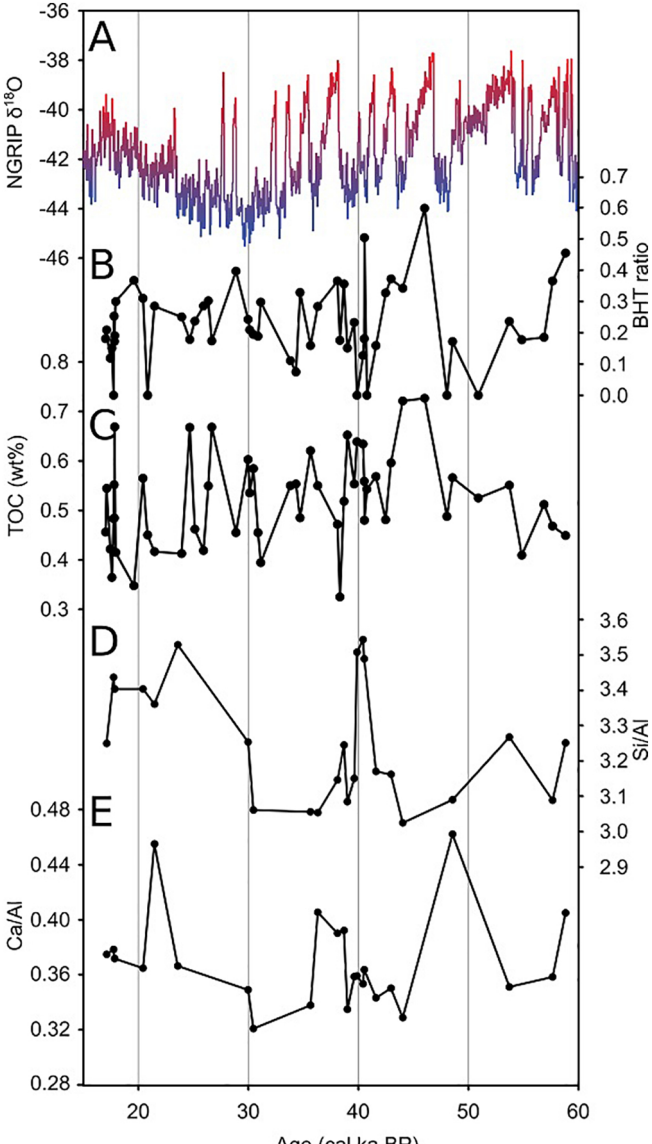
A
B
C
D
E
NGRIP δ18O
-36
-38
-40
-42
-44
-46
BHT ratio
0.7
0.6
0.5
0.4
0.3
0.2
0.1
0.0
TOC (wt%)
0.8
0.7
0.6
0.5
0.4
0.3
Si/Al
3.6
3.5
3.4
3.3
3.2
3.1
3.0
2.9
Ca/Al
0.48
0.44
0.40
0.36
0.32
0.28
20
30
40
50
60
Age (cal ka BP)

Figure 3

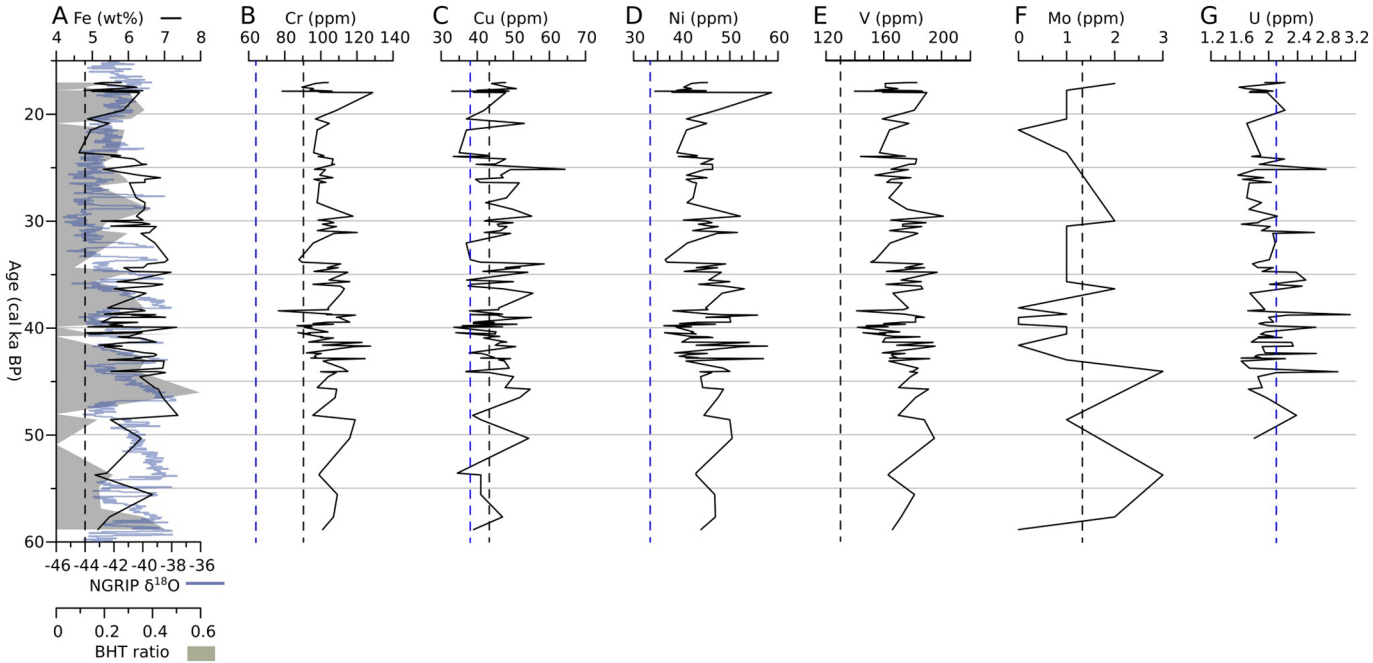
A Fe (wt%)
4 5 6 7 8
B Cr (ppm)
60 80 100 120 140
C Cu (ppm)
30 40 50 60 70
D Ni (ppm)
30 40 50 60
E V (ppm)
120 160 200
F Mo (ppm)
0 1 2 3
G U (ppm)
1.2 1.6 2 2.4 2.8 3.2
Age (cal ka BP)
20
30
40
50
60
-46 -44 -42 -40 -38 -36
NGRIP δ18O
0 0.2 0.4 0.6
BHT ratio

Figure 4

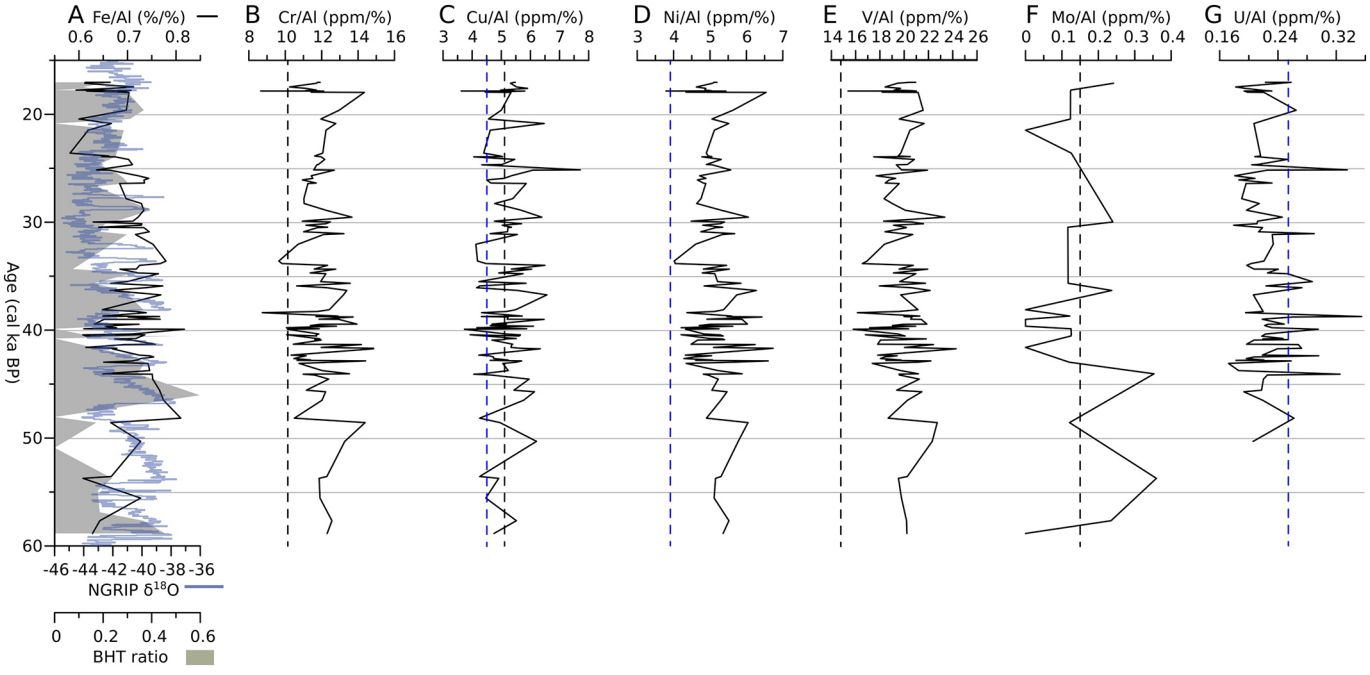
A Fe/Al (%/%)
0.6 0.7 0.8
B Cr/Al (ppm/%)
8 10 12 14 16
C Cu/Al (ppm/%)
3 4 5 6 7 8
D Ni/Al (ppm/%)
3 4 5 6 7
E V/Al (ppm/%)
14 16 18 20 22 24 26
F Mo/Al (ppm/%)
0 0.1 0.2 0.3 0.4
G U/Al (ppm/%)
0.16 0.24 0.32
Age (cal ka BP)
20
30
40
50
60
-46 -44 -42 -40 -38 -36
NGRIP δ18O
0 0.2 0.4 0.6
BHT ratio

Figure 5

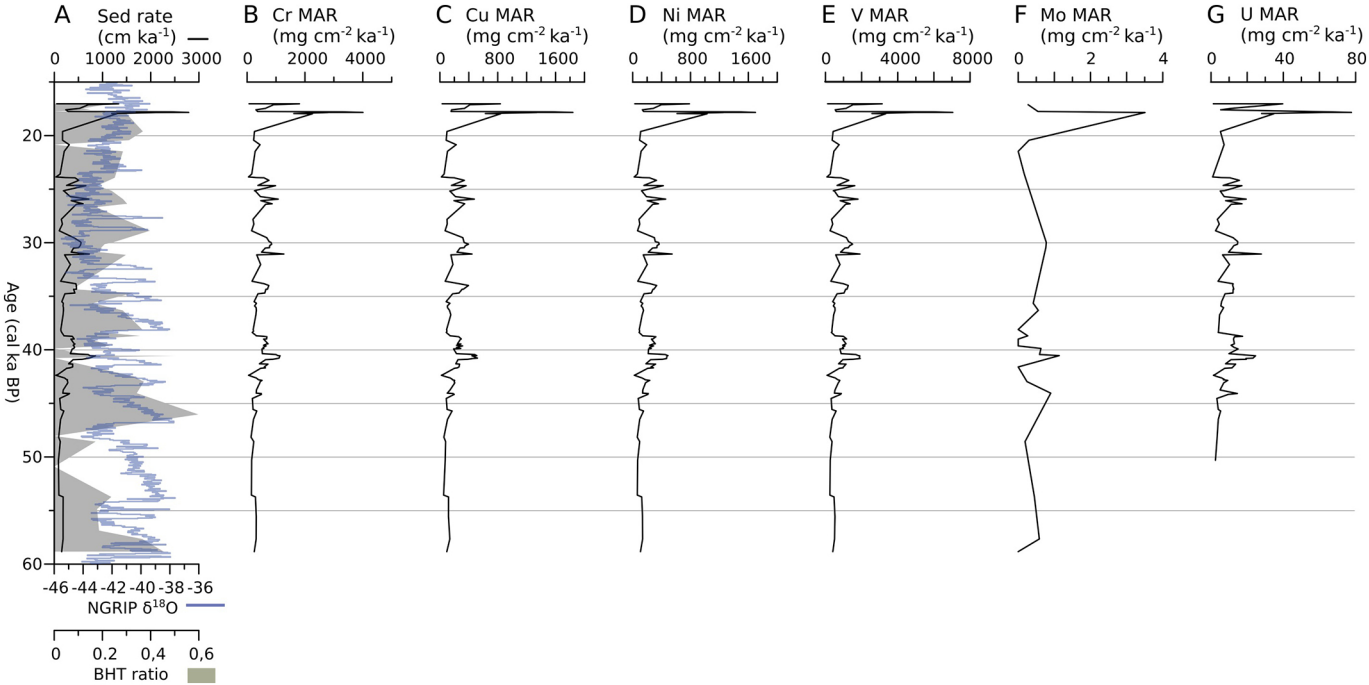

Figure 6